Hawassa University Journals - Ethiopia

Ethiopian Journal of Engineering and Technology (EJET)

Volume – 4, 2025, Pages 162 – 180. **https://doi.org/10.82127/ejet.v4i.1610**

Land Use Change Analysis Using Business as Usual Scenario of Shewa Robit Watershed, Middle Awash River Basin, Ethiopia

Ayele Desalegn Woldemariam[1] & Markos Mathewos[2,*]

[1]Institute of Geography, University of Augsburg, Augsburg, Germany.

[2]Department of Agricultural Engineering, Institute of Technology, Hawassa University, Hawassa, Ethiopia.

Corresponding Author: Markos Mathewos (godebo09@gmail.com)

Abstract

In Ethiopia, the conversion of natural vegetation cover into agricultural land is the main factor driving changes in land use and land cover (LULC). Using Landsat imagery for both historical and present-day LULC mapping and a machine learning-driven CA-Markov model was used to predict future transitions, this study examines changes in LULC in the Shewa Robit watershed. In addition, ArcGIS 10.5 was used for supervised image classification, and IDRISI Selva version 17 was used for the land change modeling and test transition probability. Significant land conversion trends, primarily a 46.46 km² increase in cultivated land at the expense of grazing and forest areas, were found in the LULC investigation undertaken between 2003 and 2023. These increases were brought about by rapid urbanization and agricultural expansion. According to the LULC projected, between 2023 and 2098, there will be a 91.4% increase in settlements and a 68.3% increase in cultivated land. This change in LULC highlights the threats to biodiversity, water resources, and soil quality that come with the fast growth of agriculture and urbanization. This study underscores the urgent need for sustainable land management practices to mitigate environmental degradation, safeguard ecosystem services, and guide future land-use planning in the watershed.

Keywords: Land Use and Land Cover Change; Machine Learning; CA-Markov Model; Landsat Imagery; Agricultural Expansion; Sustainable Land Management Practices.

1. Introduction

Land use and land cover (LULC) change in Ethiopia is primarily driven by the conversion of natural vegetation cover to use for agricultural purposes (Bewket & Abebe, 2013; Gashaw et al., 2018). With an estimated annual rate of change of 0.8% (104,600 ha yr^{-1}), the FAO (FAOSTAT, 2020) reported that Ethiopia's forest cover has fallen from 13.3% of the country's total land area (14.69 million ha) in 1993 to 11.4% of the area (12.54 million ha) in 2016 (FAOSTAT, 2020).

Changes in land use and land cover are the primary factors causing environmental changes, which are brought on by the interaction of demographic, socioeconomic, and biophysical variables (Birhanu et al., 2019; Elias et al., 2019; Guzha et al., 2018; Yesuph & Dagnew, 2019). These changes have a substantial impact on local ecosystems by modifying soil composition, decreasing vegetation cover, and altering hydrological patterns. They are caused by growing population pressures and the requirement for agricultural land to ensure food security (Genet, 2020; Hussein, 2023). These changes exacerbate the region's susceptibility to the effects of climate change and are associated with land degradation, increased soil erosion, and decreased water quality (Belay & Mengistu, 2021; Genet, 2020; Prashanth et al., 2023).

Significant LULC changes have occurred in the Shewa Robit watershed over the past few decades, resulting in a loss of biodiversity and a reduction of ecosystem services, such as carbon sequestration, water retention, and habitat provisioning for different species. Rapid deforestation and conversion of natural landscapes into agricultural land are decreasing soil fertility and increasing sedimentation in the Awash River Basin, raising concerns for long-term agricultural productivity and regional food security. Research in similar watersheds has shown that the cumulative effects of these LULC changes compromise soil and water resources, so it is crucial to comprehend current trends and predict future shifts to develop sustainable land management strategies (Aliyi, 2024; Assegide et al., 2022; Geta & Gebeyehu, 2023; Tadese et al., 2020; Tessema et al., 2020).

By examining a great deal of remote sensing data, machine learning (ML) algorithms provide sophisticated capabilities for LULC change analysis, allowing for high-resolution mapping and precise forecasts of upcoming land transitions (Birhane et al., 2024; Girma et al., 2022; Mahmoud et al., 2023; Simeon & Wana, 2024; Sisay et al., 2023; Tesfaye et al., 2024). By identifying areas at risk of degradation and directing policy interventions for ecosystem protection, these models enhance knowledge of the intricate relationships between socioeconomic and environmental drivers of land use (Hossain et al., 2024; Torabi et al., 2021). Since there is currently a lack of ML-driven analysis for LULC change prediction in Ethiopia, this effort will fill important knowledge gaps by using ML to evaluate the present and predicted LULC changes in the Shewa Robit watershed.

2. Materials and Methods

2.1 Description of the Study Area

Shewa Robit watershed is situated at 39.91°-39.95° E longitudes and 10.1º-09.96 N latitudes in Ethiopia's Amhara region, North Shewa zone (Figure 1). It is located 220 kilometers to the north of Addis Abeba, the capital of the country. Mojana Wedera Woreda, Efrata Gidim Woreda, and Simurobi Gele'alo Woreda are Shewa Robit City's neighbors to the west and south, north and east, respectively.

The watershed extends from Kewet Woreda to Mojana Wedera Woreda. The watershed is located between the Kola and high Dega agroecologies, at an altitude between 1200 and 3296 meters above sea level. But the outlet is in Shewa Robit town agro ecologically it is part of low-land (sub moist warm) areas. The watershed has a gradient that ranges from 0% to 78% slope. The watershed covers 296 km^2 area in total. The annual maximum and minimum temperature and rainfall of the Shewa Robit watershed are 32.1 and 16.1°C and 968 mm, respectively.

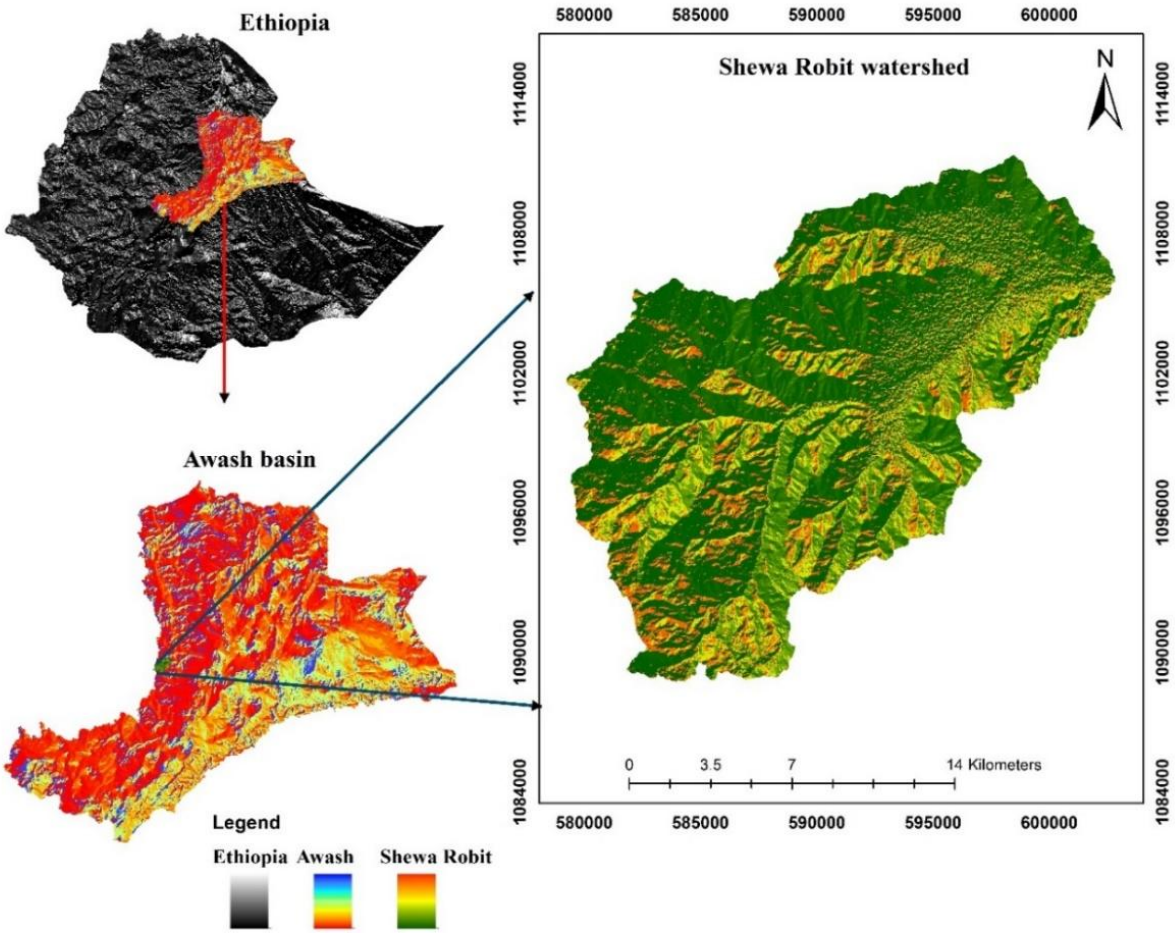

Figure 1. The location map of the study watershed

2.2. Sources of data and methods of data collection and analysis

2.2.1. Land Use Land Cover (LULC) Map

The 2023 Landsat images were used to create a baseline land use and land cover map of the watershed. It was carried out by downloading a georeferenced Landsat-9 image for the 2023 LULC classification and Landsat-7 images for the 2013 and 2003 LULC classification from USGS Earth Explorer (https://earthexplorer.usgs.gov/), which collects optical imagery with 30m spatial resolution over land and coastal waterways. After obtaining the satellite image, supervised image classification was carried out to identify the watershed's land use and land cover for the abovementioned time frames. Clear bands and images of cleared sky (0% cloud cover) were selected and composite for carrying out maximum likelihood supervised land use classification using Arc GIS 10.5 software.

2.2.2. Land Use Land Cover Classification Accuracy Assessment

The non-parametric Overall Accuracy (OA) and Kappa coefficient were computed using Equation 1-3. OA compares the number of pixels in each cell of the error matrix with the possibility of distributing pixels as a random variable (Tymków, 2009). Up to the acceptable level of accuracy, image classifications were repeated and modified. The minimum acceptable level of overall accuracy assessment is 85 % (Anderson et al., 1976).

$$\text{Overall accuracy} = \frac{\text{Total number of correctly classified pixel}}{\text{Total number of reference Pixel}} * 100\% \quad \text{Equ… 1}$$

$$\text{User accuracy} = \frac{\text{Number of correctly classified in each category}}{\text{Total Number of classified row Pixel in that category}} * 100\% \quad \text{Equ… 2}$$

$$\text{Producer accuracy} = \frac{\text{Number of correctly classified pixcel}}{\text{Number of reference Pixel in that category}*} * 100\% \quad \text{Equ… 3}$$

Kappa statistics contemplates measures of the overall accuracy of image classification and individual category accuracy as a means of actual agreement between classification and ground truth. Therefore, Kappa was computed for conformation of the accuracy of the land use land cover classification as Equation 4. A kappa coefficient value below 0.4 shows poor agreement, a value between 0.4 and 0.8 depicts moderate agreement, and a value greater than 0.8 shows strong agreement (Mishra and Rar, 2016 and Leta et al., 2021).

$$K = \frac{(\text{Observed Accuracy} - \text{Expected Accuracy})}{1 - \text{Expected Accuracy})} \quad \text{Equ... 4}$$

Where K is Kappa statistics

2.2.3 Projection of future land use and land cover

Future LULC dynamics of the study watershed were projected and modeled using TerrSet18.32 software using Land Change Modeler (LCM) and the IDRISI GIS analysis extension. CA-Markov applies a contiguity kernel to grow out a land-use map to a later period using a CA function using the anticipated amount of change that was generated by Markov chain analysis, primarily the transition probability matrices (Birhanu, 2022; Girma et al., 2022; Leta et al., 2021; Toma et al., 2023). To benefit from the advantages of combining the stochastic spatial Markov technique with the stochastic spatial CA method (Debnath et al., 2022; Hua, 2017; Nath et al., 2020), the CA-Markov model was used in this study. Depending on the previous or present land cover condition, the LULC change dynamics for any region are calculated mathematically following Equation 5 (Girma et al., 2022; Leta et al., 2021).

Since it can simulate multi-directional LULC change analysis, the CA-Markov model is commonly used and successful in detecting spatiotemporal changes in LULC (Girma et al., 2022; Mathewos et al., 2022; Toma et al., 2023). Additionally, it is a user-friendly bottom-up approach model for future LULC prediction by identification of complex system dynamics and prediction of the future spatial model by taking both physical and socioeconomic elements into account. The transition probabilities of various land cover categories from discrete time steps are quantified using it. After that, a CA model is applied to these probabilities to project spatially explicit changes over time (Mathewos et al., 2022).

$$S(t+1) = P_{ij} + S(t) \quad \text{Equ… 5}$$

Where, $S(t)$ and $S(t+1)$ are the system status at the time of t or $(t+1)$; P_{ij} is the transition probability matrix in a state which is calculated following Equation 6:

$$P_{ij} = \begin{bmatrix} P_{11} P_{12} \ldots . P_{1n} \\ P_{21} P_{22} \ldots . P_{2n} \\ \ldots \\ P_{n1} P_{n2} \ldots . P_{nn} \end{bmatrix} 0 \le P_{ij} < 1 \; and \sum_{j=1}^{n} P_{ij} = 1 \text{ , (i, j=1, 2…n)} \quad \text{Equ… 6}$$

Where P denotes the Markov probability matrix and P_{ij} is the likelihood that the current state i will change to state j in the upcoming period.

The Change Analysis, Transition Potentials, and Change Prediction tabs were the main functional keys of the Land Change Modeler (LCM). To simulate the future LULC in 2100 under the business-as-usual scenario, the change rates were established through the change analysis tab along with the transition potential maps. Maps of transition potential can be created based on the various sub-models and related explanatory variables by using a Multi-Layer Perceptron (MLP) neural network method in the LCM model. Thus, the MLP model has been used to compute the proportionate number of transitions that the dependent variables (earlier picture (2023) and later image (2100) and independent factors have on the future LULC change (Gidey et al., 2017; Girma et al., 2022; Leta et al., 2021; Mathewos et al., 2022; Moges et al., 2020; Toma et al., 2023).

Slope, altitude, aspect, distance from roads, distance from rivers, and population density are typically the main factors causing changes in land use (Birhanu, 2022). These topographic variables (Slope, altitude, and aspect) were produced using a DEM. The Euclidian distance function in Arc GIS was used to generate distance from road and river maps using vector data elements like maps of rivers and roads. The population density map of the watershed was clipped from the country's population density map. Finally, IDRISI selva Software used these variables as input to execute the potential transition maps.

3. Results and Discussions

3.1. Land Use and Climate Change Conditions of the Watershed From 2003 To 2023

The study examined the trends of land use and land cover change within the Shewa Robit watersheds over the periods of 2003 to 2013 and 2023. This study is depicted in Figure 2 and it clearly illustrates a significant shift in land use and land cover patterns over time. These changes are indicative of dynamic environmental processes and human activities within the watershed. From the Figure 2, it is evident that there have been notable alterations in land use and land cover types between 2003 and 2023.

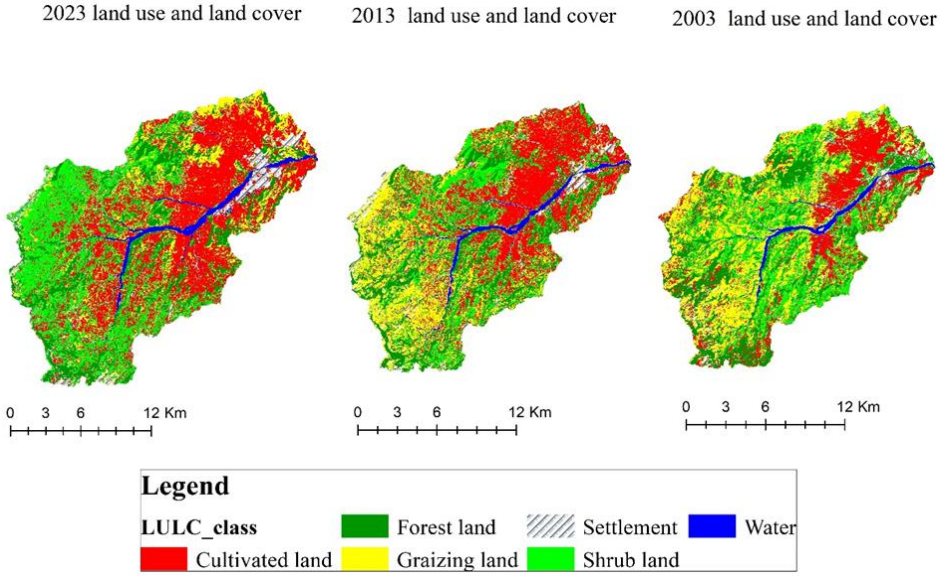

Figure 2. Land use and land cover shift from 2003 to 2023 in the Shewa Robit watershed

The land use and land cover (LULC) analysis conducted revealed insightful trends regarding the composition and changes within the watershed. Currently, the dominant land use type within the watershed is cultivated land, constituting 36.46% of the total coverage, followed by shrub land covering 24.55% of the area, as presented in Table 1. Over the period from 2003 to 2023, a positive progression was observed across all land use types, except for forest land and grazing land, which experienced decreases of 11.31 km^2 and 41.11 km^2, respectively. Notably, cultivated land exhibited the most substantial expansion, increasing by 46.46 km^2 during these 20 years. The second significant land use class showing positive progression was built-up or settlement areas, which expanded by 2.97 km^2.

This trend underscores the significant influence of increasing population demands for food and housing on the forms of land use within the watershed. The expansion of cultivated land reflects the increasing pressure on agricultural resources to meet the needs of a growing population, while the growth in built-up areas highlights the urbanization trend driven by population growth and urban development.

3.2. Gain and loss in land use and land cover types

The analysis of gains and losses in land use and land cover (LULC) over the study period, derived from the LCM change analysis module and depicted in Table 1, provides valuable insights into the dynamic nature of landscape transformations. The findings reveal significant shifts in LULC patterns, with cultivated land experiencing the largest gain while grazing, shrub, and forest cover predominantly decreased over the entire period. The net change in cultivated land reflects positive contributions from each land use and land cover type, resulting in an overall increase in cultivated land coverage. Notably, grazing land (18 km^2) and shrubland (12 km^2) were the primary contributors to this increase, underscoring their role in facilitating the expansion of cultivated areas.

Conversely, each land use and land cover type made negative contributions to the net change in forest land, leading to a decrease in forest coverage by 2013. This decline highlights the pressures on forest ecosystems, including deforestation and land conversion for various purposes. Regarding the net change in grazing land coverage, watercourses, settlements, and cultivated land (18 km^2) contributed negatively, while shrubland and forest cover also made negative contributions. This suggests a complex interplay of factors driving changes in grazing land dynamics, including land use conversion and habitat fragmentation. Shrubland, grazing land, and forest land made positive contributions to the net change in settlement coverage, indicating their role in facilitating urban expansion and infrastructure development. However, all other land use types, except for a small positive contribution by forest land, made negative contributions to the net change in shrubland coverage, resulting in a decrease in shrubland area over the study period. Remarkably, cultivated land emerged as the only land use type to make negative contributions to the net change of other land use types between the time frames studied. This suggests a pattern of land use conversion, where cultivated land encroaches on other land cover categories, leading to their decline.

The analysis of the contribution of each land use type to the net change in cultivated land between 2013 and 2023 provides valuable insights into the dynamics of land use transitions within the study area (Table 1). Similar to the contribution observed between 2003 and 2013, all land use types exhibit positive contributions to the net change in cultivated land, indicating a complex interplay of land use dynamics over the specified period. Specifically, grazing land and shrubland

emerge as the dominant land use types contributing to the increase in cultivated land coverage by 2023. With grazing land contributing 28 km² and shrub land contributing 12 km², these land use types collectively account for a significant proportion of the expansion of cultivated land within the study area.

This trend mirrors the shifting patterns observed between 2003 and 2013, where various land use types also contributed to changes in cultivated land coverage. However, the notable contributions of grazing land and shrub land to the expansion of cultivated land underscore the significant role these land use types play in facilitating land-use transitions and transformations over time.

The result of net gains from Land use land cover shifting reveals a significant expansion of cultivated land over the years, with notable changes observed between 2003 and 2023 (Table 1). In 2013, cultivated land expanded its area by a substantial 11.8%, reflecting a period of intensive growth and development in the agricultural sector. The period between 2003 and 2013 witnessed diverse contributors to the growth in coverage of cultivated land, with forest land, grazing land, and shrub land emerging as the primary sources. Forest land contributed 2.7% to agricultural expansion, followed by grazing land with 4.05% and shrub land with 5.7%. These findings suggest a significant conversion of various land types into cultivated land, possibly driven by factors such as population growth, changing agricultural practices, and economic incentives.

The period from 2013 to 2023 also revealed a continuation of agricultural expansion. Cultivated land increased by 4.4%, indicating persistent efforts to utilize more land for farming activities. This expansion of agriculture came at the expense of grazing and forest land, which experienced a decrease in coverage. Additionally, there was a notable increase in shrubland by 6.75%, suggesting a potential reversion or natural regeneration of land previously used for agriculture.

Furthermore, the observed rise in settlement areas and decline in water courses between 2013 and 2023 indicate broader changes in land use and environmental dynamics. Urbanization and infrastructure development likely drove the expansion of settlement areas, leading to further fragmentation of natural habitats and increased pressure on land resources.

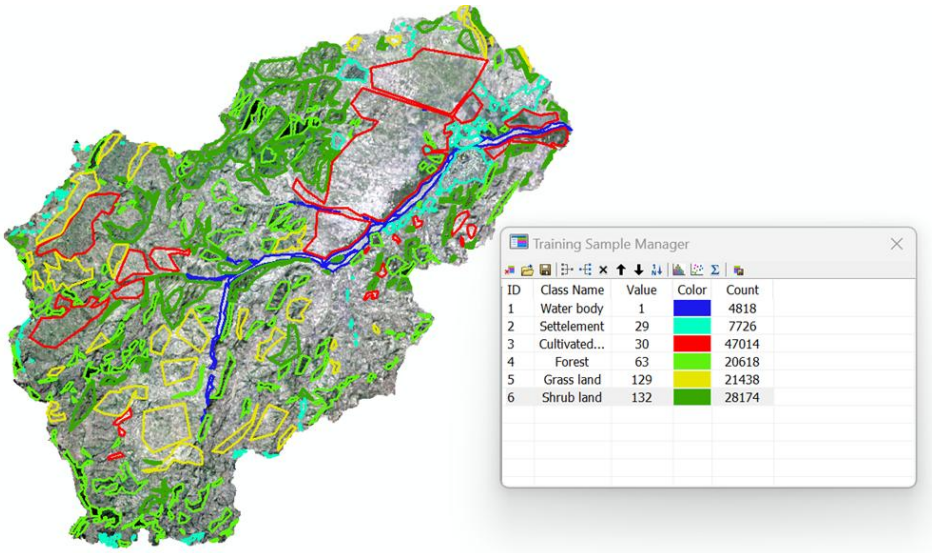

Figure 3. The detailed sampling processes of signature files during image classification.

Table 1. The types of land use, the area coverage in the watershed and the deviation due to time.

LULC Classes	2003		2013		2023		From 2013 to 2003	From 2023 to 2013	From 2023 to 2003
	Area (km^2)	Proportion (%)	Area (km^2)	Proportion (%)	Area (km^2)	Proportion (%)	km^2	km^2	km^2
Watercourse	7.33	2.48	8.69	2.93	8.39	2.83	1.36	-0.30	1.06
Forest land	58.94	19.90	50.68	17.12	47.63	16.08	-8.25	-3.05	-11.31
Settlement	19.93	6.73	21.61	7.30	22.91	7.74	1.67	1.30	2.97
Cultivated land	61.51	20.77	95.20	32.15	107.97	36.46	33.70	12.77	46.46
Shrub land	70.78	23.90	53.76	18.16	72.71	24.55	-17.01	18.95	1.93
Grazing land	77.62	26.21	66.15	22.34	36.51	12.33	-11.46	-29.64	-41.11
Total	296.1	100	296.1	100	296.1	100			

Procedures were followed to create signature files for each watershed's land use type, as described in Figure 3, which served as an input for maximum likelihood image analysis during supervised image classification in the Arc GIS environment. As seen in the picture below, comprehensive signature files were obtained throughout the land use and land cover classification. To accurately classify the land use type in supervised image classification, it was crucial to obtain as many signature files as possible (Lu & Weng, 2007).

3.3 Land Use Land Cover Classification Accuracy Assessment

To ensure the validation of the land use and land cover (LULC) analysis, an accuracy assessment was conducted using 205 reference points. These reference points were distributed across the watershed and were verified using Google Earth imagery for each respective time frame. The distribution of these sampling points throughout the watershed is depicted in Figure 4.

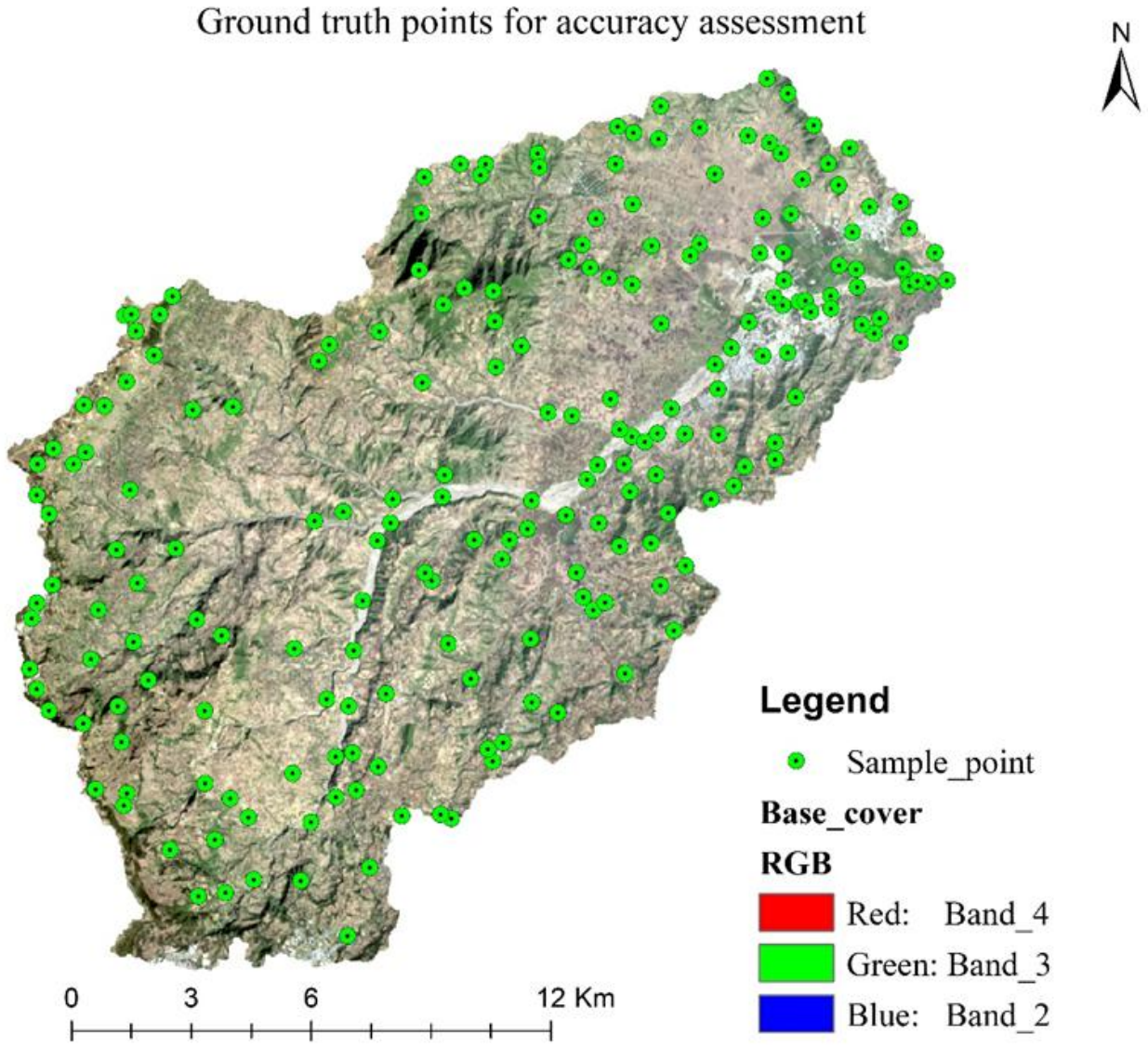

Figure 4. The 205 sampling points used for accuracy assessment during LULC classification

The following quality assessment findings were ultimately obtained following the aforementioned procedures (Table 2). After an extensive investigation, all land use and land cover classifications in all periods could reach the following good quality assessment parameters results:

Table 2. LULC classification accuracy assessment matrix for the years 2003, 2013, and 2023.

No.	LULC class	2003		2013		2023	
		PA (%)	UA (%)	PA (%)	UA (%)	PA (%)	UA (%)
1	Cultivated land	95	93	87.8	92.3	85.7	100
2	Forest land	93	93	77.8	84.8	74.4	97
3	Grazing land	79	95	83.9	76.5	77.8	67.7
4	Watercourse	100	100	100	100	100	94.4
5	Settlement	100	100	100	93.8	97.1	87.2
6	Shrubland	90	72	81.3	81.3	91.7	73.3
7	OA (%)	91.71		88.29		87.32	
8	KC (%)	90.08		86.25		85.07	
OA: Overall Accuracy, KC: Kappa coefficient, PA: Producer Accuracy & UA: User Accuracy							

3.4 Projected LULC Conditions from 2024 to 2098

3.4.1 Input for Land Use Land Cover Projection

The key factors (Table 3 and Figure 5) considered for land cover projection included elevation, slope, distance from the roads, distance from the rivers, and population density maps. The analysis revealed that elevation was the primary driving variable (Cramer's V of 0.2298) influencing changes in projected land use and land cover types, while slope exhibited the least impact (Cramer's V of 0.0261). In contrast, the study at the Gidabo river basin, the main Ethiopian rift reported slope as the second most driving variable and elevation as the least influential variable (Girma et al., 2022). Another study at Matenchose Watershed, Rift Valley Basin of Ethiopia found population density as the important driving variable while slope was the least influential driving variable that impacts LULCC in the study watershed (Mathewos et al., 2022).

Table 3. The drivers' variables that are assumed to drive the land use change in the future

No.	LULC Driving Variables	Cramer's V
1	Elevation	0.2298
2	Slope	0.0261
3	Distance from the road	0.1249
4	Distance from river	0.1847
5	Population density	0.1324

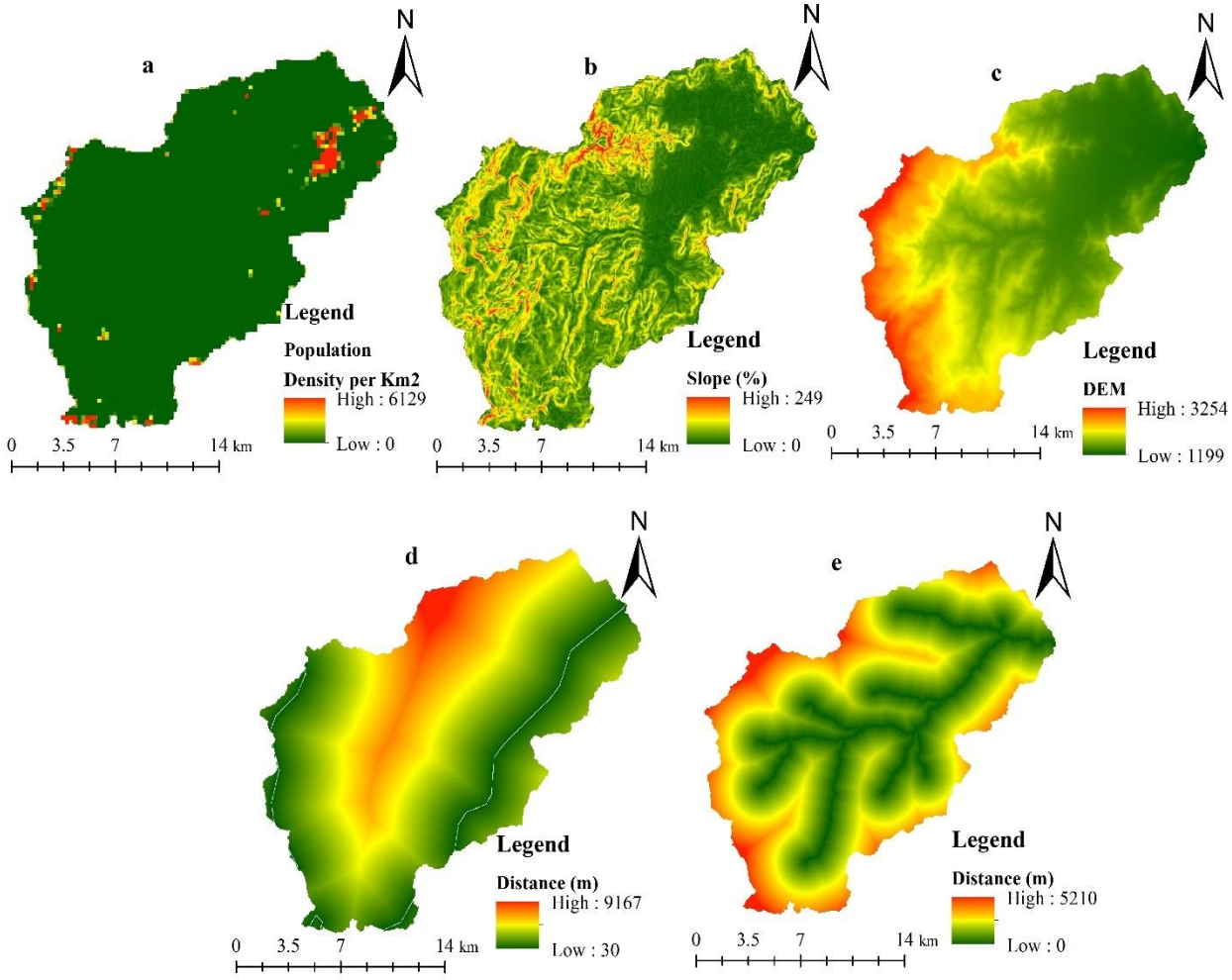

Figure 5. Driving variables for the FLULC: (a) population density map, (b) slope map, (c) Elevation map, (d) distance from the roads map, and (e) distance from rivers map.

3.4.2 Accuracy Assessment for The Projected Land Use And Land Cover

The comparison between the actual land use of 2023 and the simulated 2023 land use based on the CA-Markov model provides valuable insights into the accuracy and validity of the model's predictions.

Kappa coefficient of agreement: <0 denotes less than chance agreement, 0.01-0.40 poor agreement, 0.41-0.6 moderate agreement, 0.61-0.80 substantial agreement, and 0.81-1.00 nearly perfect agreement. These statistics, which are adjusted for accuracy by chance, gauge the goodness of fit between the model's predictions and reality (Mukherjee et al., 2009). The agreement/disagreement components (Table 4) are validated through a validation analysis conducted by the Clark Lab's LCM module of IDRISI Selva version 17.00 software. The results are further divided into two categories: 0.0668 (error due to quantity/DisagreeQuantity) and 0.2149 (error due to allocation/disagree gridcell). Therefore, the data table showed that rather than quantity error between the projected and actual 2023 images, allocation error was the cause of the differences between the two maps.

Table 4. Results of validation analysis of two images (Agreement / Disagreement components values)

Agreement / Disagreement	Value (%)
Agreement Chance	14.29
Agreement Quantity	13.43
Agreement Strata	0.00
Agreement Gridcell	44.12
Disagree Gridcell	21.49
Disagree Strata	0.00
Disagree Quantity	6.68

In assessing the accuracy and validity of predictions made using the CA-Markov model for land use and land cover (LULC) changes, several indices of agreement are employed, notably the Kno index and the Klocation index (Table 5). The Kno index, derived from the conventional Kappa index of agreement, serves as a robust metric for determining the overall accuracy of the prediction generated by the CA-Markov model. This index provides insight into the degree of agreement between the simulated LULC map and the actual observed LULC map. Additionally, the Klocation index contributes to validating the simulation's location predictions, offering assurance regarding the spatial accuracy of the model's outputs.

Upon analyzing the results displayed in the table containing these indices of agreement, it becomes apparent that the simulated and actual images exhibit a considerable level of concordance. The average value of these indices, standing at 0.657, signifies that more than 65.7% of the LULC categories between the two images are equivalent.

This level of agreement suggests that the CA-Markov model demonstrates a commendable capability in predicting LULC changes within the study area. The high level of consistency between the simulated and actual images indicates the model's efficacy in capturing and replicating the complex dynamics of land use and cover transitions over time. Overall, the substantial agreement between the simulated and actual LULC images, as indicated by the Kno index and Klocation index, underscores the reliability of the CA-Markov model in predicting future land use dynamics within the study area.

Table 5. Accuracy assessment of the simulated land use image of 2023.

Index	Value
Kno	0.6714
Klocation	0.6725
KlocationStrata	0.6725
Kstandard	0.6103

3.5 Projected Land Use and Land Cover (LULC)

Following the successful simulation of Land Use and Land Cover (LULC) changes in 2023, the subsequent figures (Figure 6) depicting the Future Land Use and Land Cover Change (FLULCC) for the periods of 2023, 2060, and 2098 reveal intriguing insights into the evolution of land use patterns over time. Notably, these figures illustrate a significant shift in land cover categories, particularly in regions previously shaded green (forest and shrub) and yellow (grazing) in the western and southern areas, which gradually transition towards red (cultivated) and grey strip shaded (settlement) as the end of the century.

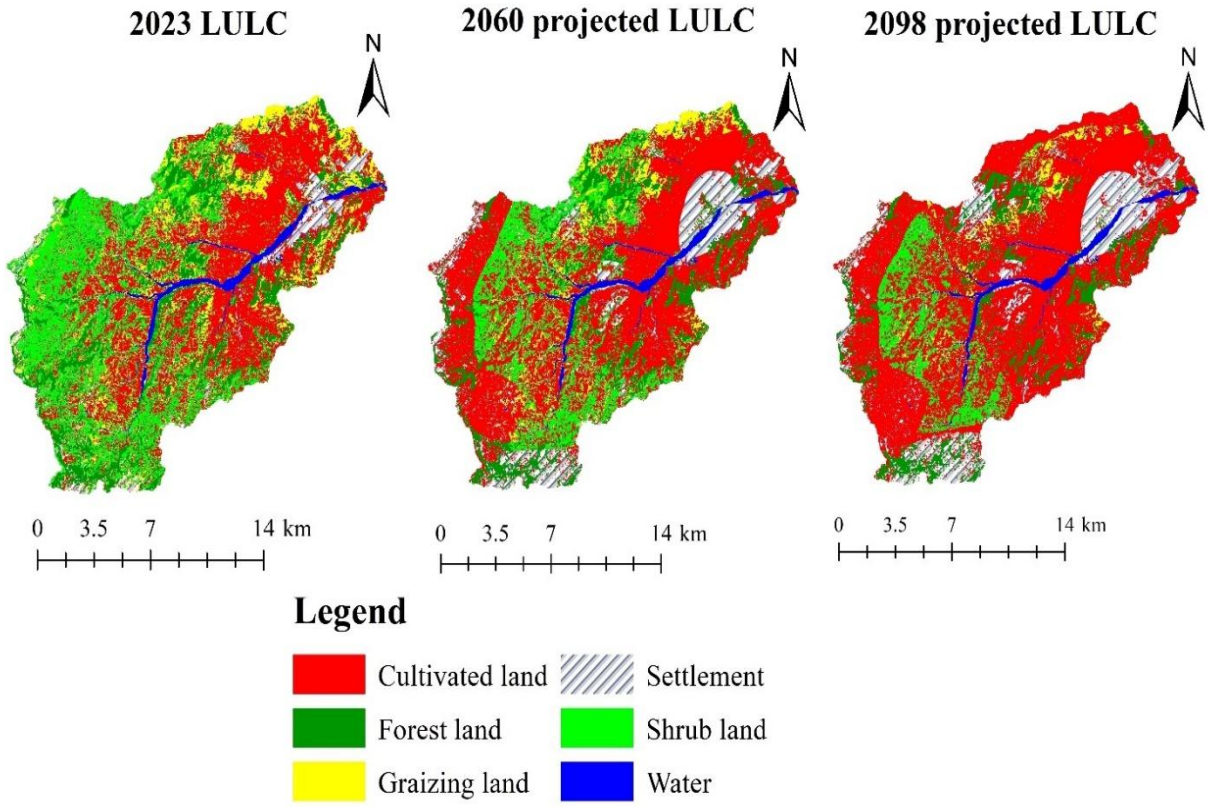

Figure 6. The land use and land cover shifts running for 75 years ahead from 2023 to 2098

The Shewa Robit watershed is undergoing a significant temporal transition in land use and cover, as depicted in Table 6. The projection indicates a profound shift in the landscape dynamics, with cultivated or settlement areas emerging as the predominant land use type. It suggests a substantial 91.4% increase in settlement land use change over the next 75 years. Looking ahead to the end of the century, it becomes evident that cultivated land was witness a staggering 68.3% increase, cementing its status as the second most prevalent land use type. The study conducted in the Fincha'a watershed revealed a noticeable trend of expanding cultivated land, settlement areas, and water bodies at the detriment of forest land, shrub land, and grassland from 1991 to 2021 (Takala & Kabite, 2023). Similarly, between 2028 and 2048, barren land, built-up areas, and cultivated land were documented to increase, leading to the depletion of water bodies, forests, shrub-bush, and plantation land (Entahabu et al., 2023).

The increase in the coverage of settlements and cultivated land poses significant challenges, particularly in balancing the needs of urban development with environmental preservation. Surprisingly, projections suggest that this issue might exacerbate more in the mid-future compared to the far future, primarily due to the shaping of societal mindsets regarding environmental concerns and urban expansion.

Table 6. The area coverage of each land use and land cover from 2023 to 2098 and their shift in time.

No.	LULC class	Area (km^2) of each year			Shift in coverage from one year to the other in km^2 (%)		
		2023	2060	2098	2023 to 2060	2060 to 2098	2023 to 2098
1	Settlement	22.91	38.28	43.83	15.4 (67.1)	5.55 (14.5)	20.9 (91.4)
2	Watercourse	8.39	8.23	8.12	-0.2 (-1.9)	-0.1 (-1.4)	-0.3 (-3.3)
3	Cultivated land	107.97	147.47	181.76	39.5 (36.6)	34.3 (23.2)	73.8 (68.3)
4	Forest land	47.63	37.20	27.90	-10.4 (-21.9)	-9.3 (-25)	-19.7 (-41.4)
5	Shrub land	72.71	46.25	25.90	-26.5 (-36.4)	-20.4 (-44)	-46.9 (-64.4)
6	Grazing land	36.51	18.43	8.22	-18.1 (-49.5)	-10.2 (-55.4)	-28.3 (-77.5)

In the mid-future, which spans the next few decades (by 2060), societal attitudes toward environmental conservation and urban development are poised to play a pivotal role in exacerbating the expansion of settlements and cultivated land. Numerous studies have consistently highlighted the trend of increasing cultivated land, settlements, and in some cases, water bodies, at the expense of forest land, shrubland, and grasslands (Entahabu et al., 2023; Girma et al., 2022; Leta et al., 2021; Mathewos et al., 2022; Nath et al., 2020; Sisay et al., 2023; Yesuph & Dagnew, 2019). For instance, in the Matenchose watershed, cultivated land and settlement areas experienced significant expansions of 139.4% and 360%, respectively (Mathewos et al., 2022). Similarly, Girma et al. (2022) noted substantial gains in agricultural land, settlements, and water bodies, accompanied by losses in forests, shrubs, and grasslands. Predictions of land use and land cover (LULC) changes between 2035 and 2055 revealed further increases in agricultural land, grassland, settlement areas, and woodlands by 44.02%, 30.35%, 69.2%, and 55.05%, respectively, while forest and scrub/bush lands experienced declines of 21.53% and 11.08%, respectively (Abdule et al., 2023).

Conversely, the current coverage of grazing areas and shrublands is anticipated to experience marked declines by 2098. Projections indicate a substantial 77.5% decrease in grazing areas and a notable 64.4% reduction in shrubland coverage. The study by Mathewos et al. (2022) also reported the decline of grassland, bare land, and forestland by 77.36%, 81.01%, and 6.26%, respectively by 2050. These declines underscore the environmental pressures and land-use practices that are reshaping the natural habitats within the watershed. On the adverse side of the land cover shift, grazing land and shrub land emerged as the primary land use types experiencing substantial reductions. From 2023 to 2098, grazing land decreased by 28.3 km^2 (-77.5%), while shrubland diminished by 46.9 km^2 (-64.4%). A parallel observation was made by Toma et al. (2023), who reported similar findings, indicating that cultivated land, built-up areas, and bare land expanded at the cost of shrubland and forest land.

4. Conclusion and Recommendation

This study concludes that agricultural and settlement areas are expanding at the expense of natural landscapes, while forests and grasslands are experiencing major reductions. These trends are predicted to continue by the CA-Markov model, which predicts that by 2098, cultivated and settlement areas will account for the majority of the watershed, growing by 68.3% and 91.4%, respectively. Such alterations have significant implications for the soil integrity, hydrology, and biodiversity of the area. Rapid LULC shifts may worsen land degradation and water quality problems, which are vital for regional agricultural and community resilience, as well as endanger ecological services like carbon sequestration and water retention. Immediate action through sustainable land use policies and restoration projects is necessary to avert further degradation and maintain the agricultural and environmental stability of the watershed. Additionally, more studies about how to incorporate climate data into LULC models would enhance adaptive strategies to manage the combined impacts of land use changes and climatic stresses on this ecosystem.

Funding

No Funding has been received.

Competing Interests

The authors declare no competing interests.

Concerns to Publish

All the authors concern to the publication of this article.

References

Abdule, A. M., Muluneh, A., & Woldemichael, A. (2023). Impact of Climate and Land Use / Cover Changes on Streamflow in Yadot Watershed, Genale Dawa Basin , Ethiopia. https://doi.org/10.1177/11786221231200106

Aliyi, M. M. (2024). Impact of Land use Land cover changes on surface water resources in the Laga-Arba watershed, Awash River basin, Ethiopia, 7. https://doi.org/10.13140/RG.2.2.28071.15525

Anderson, J. R., Hardy, E. E., Roach, J. T., & Witmer, R. E. (1976). A Land Use And Land Cover Classification System For Use With Remote Sensor Data. Geological Survey Professional Paper 964, 34.

Assegide, E., Alamirew, T., Bayabil, H., & Dile, Y. T. (2022). Impacts of Surface Water Quality in the Awash River Basin , Ethiopia : A Systematic Review. Frontiers in Water, 3(3). https://doi.org/10.3389/frwa.2021.790900

Belay, T., & Mengistu, D. A. (2021). Impacts of land use/land cover and climate changes on soil erosion in Muga watershed, Upper Blue Nile basin (Abay), Ethiopia. Ecological Processes, 10(1). https://doi.org/10.1186/s13717-021-00339-9

Bewket, W., & Abebe, S. (2013). Land-use and land-cover change and its environmental implications in a tropical highland watershed, Ethiopia. International Journal of Environmental Studies, 70(1): 126–139. https://doi.org/10.1080/00207233.2012.755765

Birhane, E., Negash, E., Getachew, T., Gebrewahed, H., Gidey, E., Gebremedhin, M. A., & Mhangara, P. (2024). Changes in total and per - capital ecosystem service value in response to land - use land - cover dynamics in north - central Ethiopia. Scientific Reports, 14, 1–14. https://doi.org/10.1038/s41598-024-57151-6

Birhanu, A., Masih, I., van der Zaag, P., Nyssen, J., & Cai, X. (2019). Impacts of land use and land cover changes on hydrology of the Gumara catchment, Ethiopia. Physics and Chemistry of the Earth, 112: 165–174. https://doi.org/10.1016/j.pce.2019.01.006

Birhanu Wolde Gindi. (2022). Impact of Land Use/Land Cover and Climate Change on Soil Erosion in Sile Watershed, Lake Abaya-Chamo Sub- Basin, Southern Ethiopia. Hawassa University.

Debnath, J., Sahariah, D., Lahon, D., Nath, N., Chand, K., Meraj, G., Farooq, M., Kumar, P., Kanga, S., & Singh, S. K. (2022). Geospatial modeling to assess the past and future land use-land cover changes in the Brahmaputra Valley, NE India, for sustainable land resource management. Environmental Science and Pollution Research, November. https://doi.org/10.1007/s11356-022-24248-2

Elias, E., Seifu, W., Tesfaye, B., & Girmay, W. (2019). Impact of land use/cover changes on lake ecosystem of Ethiopia central rift valley. Cogent Food and Agriculture, 5(1). https://doi.org/10.1080/23311932.2019.1595876

Entahabu, H. H., Minale, A. S., & Birhane, E. (2023). Modeling and Predicting Land Use/Land Cover Change Using the Land Change Modeler in the Suluh River Basin, Northern Highlands of Ethiopia. Sustainability (Switzerland), 15(10): 21–25. https://doi.org/10.3390/su15108202

FAOSTAT. (2020). Food and Agriculture Organization Corporate Statistical Database. https://en.wikipedia.org/wiki/Food_and_Agriculture_Organization_Corporate_Statistical_Database

Gashaw, T., Tulu, T., Argaw, M., & Worqlul, A. W. (2018). Modeling the hydrological impacts of land use/land cover changes in the Andassa watershed, Blue Nile Basin, Ethiopia. Science of the Total Environment, 619: 1394–1408. https://doi.org/10.1016/j.scitotenv.2017.11.191

Genet, A. (2020). Population Growth and Land Use Land Cover Change Scenario in Ethiopia. International Journal of Environmental Protection and Policy, 8(4): 77–85. https://doi.org/10.11648/j.ijepp.20200804.12

Geta, B., & Gebeyehu, A. (2023). Evaluating the impact of land use and land cover changes on sediment yield dynamics in the upper Awash basin , Ethiopia the case of Koka reservoir. Heliyon, 9(12), e23049. https://doi.org/10.1016/j.heliyon.2023.e23049

Gidey, E., Dikinya, O., Sebego, R., Segosebe, E., & Zenebe, A. (2017). Cellular automata and Markov Chain (CA_Markov) model-based predictions of future land use and land cover scenarios (2015–2033) in Raya, northern Ethiopia. Modeling Earth Systems and Environment, 3(4): 1245–1262. https://doi.org/10.1007/s40808-017-0397-6

Girma, R., Fürst, C., & Moges, A. (2022). Land use land cover change modeling by integrating artificial neural network with cellular Automata-Markov chain model in Gidabo river basin, main Ethiopian rift. Environmental Challenges, 6: 100-119. https://doi.org/10.1016/j.envc.2021.100419

Guzha, A. C., Rufino, M. C., Okoth, S., Jacobs, S., & Nóbrega, R. L. B. (2018). Impacts of land use and land cover change on surface runoff, discharge and low flows: Evidence from East Africa. Journal of Hydrology: Regional Studies, 15: 49–67. https://doi.org/10.1016/j.ejrh.2017.11.005

Hossain, M., Wiegand, B., Reza, A., Chaudhuri, H., Mukhopadhyay, A., Yadav, A., & Kumar, P. (2024). A machine learning approach to investigate the impact of land use land cover (LULC) changes on groundwater quality , health risks and ecological risks through GIS and response surface methodology (RSM). Journal of Environmental Management, 366(5): 121911. https://doi.org/10.1016/j.jenvman.2024.121911

Hua, A. K. (2017). Application of CA-Markov model and land use/land cover changes in Malacca river watershed, Malaysia. Applied Ecology and Environmental Research, 15(4): 605–622. https://doi.org/10.15666/aeer/1504_605622

Hussein, A. (2023). Impacts of Land Use and Land Cover Change on Vegetation Diversity of Tropical Highland in Ethiopia. Applied and Environmental Soil Science. https://doi.org/10.1155/2023/2531241

Leta, M. K., Demissie, T. A., & Tränckner, J. (2021). Modeling and prediction of land use land cover change dynamics based on land change modeler (Lcm) in nashe watershed, upper blue nile basin, Ethiopia. Sustainability, 13(7). https://doi.org/10.3390/su13073740

Lu, D., & Weng, Q. (2007). A survey of image classification methods and techniques for improving classification performance. International Journal of Remote Sensing, 28(5): 823–870. https://doi.org/10.1080/01431160600746456

Mahmoud, R., Hassanin, M., Feel, H. Al, & Badry, R. M. (2023). Machine Learning-Based Land Use and Land Cover Mapping Using Multi-Spectral Satellite Imagery: A Case Study in Egypt. 1–21.

Mathewos, M., Lencha, S. M., & Tsegaye, M. (2022). Land Use and Land Cover Change Assessment and Future Predictions in the Matenchose Watershed, Rift Valley Basin, Using CA-Markov Simulation. Land, 11(10). https://doi.org/10.3390/land11101632

Mishra, V.N.; Rai, P. . (2016). A remote sensing aided multi-layer perceptron-Markov chain analysis for land use and land cover change prediction in Patna district (Bihar), India. Arab. J. Geosci., 9: 1–18.

Moges, D. M., Kmoch, A., Bhat, H. G., & Uuemaa, E. (2020). Future soil loss in highland Ethiopia under changing climate and land use. Regional Environmental Change, 20(1): 1–14. https://doi.org/10.1007/s10113-020-01617-6

Mukherjee, S., Shashtri, S., Singh, C. K., Srivastava, P. K., & Gupta, M. (2009). Effect of canal on land use/land cover using remote sensing and GIS. Journal of the Indian Society of Remote Sensing, 37(3): 527–537. https://doi.org/10.1007/s12524-009-0042-6

Nath, B., Wang, Z., Ge, Y., Islam, K., Singh, R. P., & Niu, Z. (2020). Land use and land cover change modeling and future potential landscape risk assessment using Markov-CA model and analytical hierarchy process. ISPRS International Journal of Geo-Information, 9(2). https://doi.org/10.3390/ijgi9020134

Prashanth, M., Kumar, A., Dhar, S., & Verma, O. (2023). Land use / land cover change and its implication on soil erosion in an ecologically sensitive Himachal Himalayan watershed , Northern. 2: 1–17. https://doi.org/10.3389/ffgc.2023.1124677

Simeon, M., & Wana, D. (2024). Impacts of Land use Land cover dynamics on Ecosystem services in maze national park and its environs , southwestern Ethiopia. Heliyon, 10(9), e30704. https://doi.org/10.1016/j.heliyon.2024.e30704

Sisay, G., Gesesse, B., Fürst, C., Kassie, M., & Kebede, B. (2023). Modeling of land use/land cover dynamics using artificial neural network and cellular automata Markov chain algorithms in Goang watershed, Ethiopia. Heliyon, 9(9), e20088. https://doi.org/10.1016/j.heliyon.2023.e20088

Tadese, M., Kumar, L., Koech, R., & Kogo, B. K. (2020). Remote Sensing Applications : Society and Environment Mapping of land-use / land-cover changes and its dynamics in Awash River Basin using remote sensing and GIS. Remote Sensing Applications: Society and Environment, 19(7), 100352. https://doi.org/10.1016/j.rsase.2020.100352

Takala, A., & Kabite, G. (2023). Responses of soil erosion and sediment yield to land use / land cover changes : In the case of Fincha ' a watershed , upper Blue Nile Basin , Ethiopia. Environmental Challenges, 13(11), 100789. https://doi.org/10.1016/j.envc.2023.100789

Tesfaye, W., Elias, E., Warkineh, B., Tekalign, M., & Abebe, G. (2024). Modeling of land use and land cover changes using google earth engine and machine learning approach : implications for landscape management. Environmental Systems Research, 13(31).

Tessema, N., Kebede, A., & Yadeta, D. (2020). Modeling land use dynamics in the Kesem sub-basin , Awash River basin , Ethiopia Modeling land use dynamics in the Kesem sub-basin , Awash River basin , Ethiopia. Cogent Environmental Science, 6(1). https://doi.org/10.1080/23311843.2020.1782006

Toma, M. B., Belete, M. D., & Ulsido, M. D. (2023). Historical and future dynamics of land use land cover and its drivers in Ajora-Woybo watershed, Omo-Gibe basin, Ethiopia. Natural Resource Modeling, 36(1). https://doi.org/10.1111/nrm.12353

Torabi, A., Hamid, H., Zahra, D., Ali, K., Davudirad, A., & Rouzbeh, S. (2021). Land degradation risk mapping using topographic , human - induced , and geo - environmental variables and machine learning algorithms , for the Pole - Doab watershed , Iran. Environmental Earth Sciences, 80(1): 1–21. https://doi.org/10.1007/s12665-020-09327-2

Tymków P. (2009). Application of photogrammetric and remote sensing methods for identification of resistance coefficients of high water flow in river valleys.

Yesuph, A. Y., & Dagnew, A. B. (2019). Land use/cover spatiotemporal dynamics, driving forces and implications at the Beshillo catchment of the Blue Nile Basin, North Eastern Highlands of Ethiopia. Environmental Systems Research, 8(1). https://doi.org/10.1186/s40068-019-0148-y